Using Computational Fluid Dynamics to investigate heat exchanges between the environment and photovoltaic panels

Thauã A. da G. Santos[1], Nuccia C. A de Sousa[2]

[1]*Department of Production Engineering, Federal University of Alagoas – Arapiraca Campus*
Av. Beira Rio, S/N, Penedo, 57200-000, Alagoas, Brazil
thaua.santos@arapiraca.ufal.br
[2]*Department of Production Engineering, Federal University of Alagoas – Arapiraca Campus*
Av. Beira Rio, S/N, Penedo, 57200-000, Alagoas, Brazil
nuccia.sousa@penedo.ufal.br

Abstract. This study aims to investigate natural convection heat exchanges between photovoltaic panels and the external environment through Computational Fluid Dynamics (CFD) using the open-source software OpenFOAM, excluding heat transfer by radiation. We sought to evaluate the effects that varying the plate inclination causes on the ambient temperature. The study is relevant because temperature impacts the efficiency of photovoltaic systems, as well as heat exchange with the environment. We developed the modeling in three stages: pre-processing, where Gmsh software was used for creating the geometric model and discretization, forming the computational mesh; processing, where OpenFOAM uses the buoyantPimpleFoam solver to resolve the governing fluid equations via the Finite Volume Method to acquire the variables of interest; and post-processing, where Paraview supported the visualization of results. Temperature and velocity fields were mapped, and the results show the formation of air flows and the gradual propagation of temperature to the environment from the panel through thermal plumes. We found that increasing the panel's inclination contributes to an increase in the average temperature in the environment above the photovoltaic panel.

Keywords: Natural Convection, Computational Fluid Dynamics, OpenFOAM.

1 Introduction

Solar energy is an alternative to the growing demand for energy over time, given the growing concern for the environment. Solar sources can play an important role in diversifying the exploration of energy sources, in the use of renewable sources, in reducing carbon dioxide emissions in the generation process and in increasing the resilience of the Brazilian electrical matrix, which is currently made up mainly of power plants hydroelectric plants [1]. The conversion of solar energy into electrical energy is based on the photovoltaic effect. However, only part of the electromagnetic radiation from the sun is converted into electrical energy, the rest is reflected or transferred to the environment in the form of heat, causing an increase in the temperature of the plate and the occurrence of heat exchange with the environment [2].

The heat transfer processes involved in the energy balance of solar panels are relevant in the analysis of photovoltaic systems due to the influence that temperature has on the efficiency of the panels, which in turn affects the electrical power supplied by these systems. As noted by Saleem et al. [3] and Amelia et al. [4], the authors found that an increase in temperature leads to a reduction in the power output. Therefore, it is preferable to lower the panel's temperature by increasing the heat transfer rate to the external environment.

This phenomenon drives studies like those of Nižetić et al. [5], who proposed structural modifications and numerically investigated the effects on reducing the temperature of specific layers of the PV panel, achieving a reduction of about 4 °C with slits on the front surface. The primary heat transfer mechanism in these scenarios is natural convection, a phenomenon extensively studied in the literature with various empirical correlations to quantify the heat transfer coefficient. For example, the works of Fan et al. [6], which provides a literature review on fundamental topics, and Jaffer [7], who aimed to validate new formulas to predict heat transfer by natural convection from isothermal plates.

In this study, we will address heat exchange by natural convection in a photovoltaic panel simplified by the flat plate model, aiming to evaluate the effects that variations in the plate's inclination relative to the surface have on heat transfer. CFD modeling was performed using open-source software, including OpenFOAM – a program based on a set of modules written in C++ language, open-source, with the physical fluid model equations discretized by the Finite Volume Method, standing out among other well-established commercial CFD software such as ANSYS and COMSOL [8].

2 Methodology

Fluid dynamics is modeled by the physical laws of conservation of mass, momentum, and energy, which are expressed in nonlinear partial differential equations, presented in their general form in eq. (1), eq. (2), and eq. (3), respectively. Although analytical solutions for these equations are known for a limited number of simplified cases, numerical solutions for fluid flow have gained prominence with advances in the field of CFD [9].

$$\frac{\partial \rho}{\partial t} + \nabla \cdot (\rho V) = 0 \tag{1}$$

where ρ is the density of the fluid and V is the velocity vector.

$$\rho \frac{\mathrm{d}V}{\mathrm{d}t} = \rho g - \nabla p + \nabla \cdot \tau_{ij} \tag{2}$$

where g is the acceleration of gravity, ∇p is the pressure gradient and τij is the viscous stress tensor.

$$\rho c_p \frac{DT}{Dt} = \nabla . (K \nabla T) + q''' + \beta T \frac{DP}{Dt} + \mu \Phi \tag{3}$$

where cp is the specific heat at constant pressure of the fluid, T is the temperature, K is the coefficient of thermal conductivity of the fluid, q''' is the heat flow per unit volume, β is the coefficient of volumetric expansion of the fluid, μ is the dynamic viscosity of the fluid and Φ is the viscous dissipation function.

The conservation equations are grouped into a general transport equation for the variable of interest, eq. (4), composed of four terms: temporal, advective, diffusive, and source term. Here, Φ is the variable of interest, Γ is the diffusion coefficient, and S is the source term.

$$\frac{\partial}{\partial t} \int_v \rho \phi \partial V + \oint_A \rho \phi V . \partial A = \oint_A \Gamma_\phi \nabla \phi . \partial A + \int_v S_\phi \partial V \tag{4}$$

OpenFOAM uses the Finite Volume Method for the discretization of the governing equations. This method is based on decomposing the domain into a finite number of small control volumes where the value of the flow variables is stored at the centroid of each volume. The conservation equations are described in their integral form for each volume and converted into surface integrals. Then, interpolation is used to approximate the variation of the variables within the control volume and to relate the flux values at the face centroids. The partial differential equations are thus approximated by a set of linear algebraic equations summing the fluxes of the variables at the faces of each control volume, which can be solved numerically [10].

CFD modeling consists of three stages: pre-processing, processing, and post-processing. The pre-processing stage begins with the computational representation of the studied physical phenomenon, which involves creating a geometric model using CAD (Computer Aided Design) software. To reduce the computational cost of the simulation, a simplified two-dimensional model, a pseudo-3D, was considered since OpenFOAM only works in three-dimensional coordinates. Subsequently, the domain is discretized by generating a finite volume mesh with appropriate refinement in the areas of interest of the flow. Additionally, the initial and boundary conditions of the problem are defined.

The open-source software Gmsh [11]was used for creating the geometry and subsequently generating the finite volume mesh. This choice was made because Gmsh allows users the freedom to choose the number of mesh divisions along each line of the geometric surface. OpenFOAM includes a range of utilities that enable users to use external CAD software and mesh generators, exporting the discretized model to the desired format.

An unstructured mesh composed of triangular prisms and layers of hexahedra with progressive refinement near the flat plate was generated. This refinement was necessary to obtain better results for the thermal boundary layer, where a high temperature gradient in the flow is expected. Four regions of the domain were defined: front and back, plate, ground, and external environment. Wall conditions were assigned to the floor and plate regions, empty-type conditions to the front and back region, and free flow conditions to the external environment region, allowing the free passage of mass to the sides and tops of the domain.

The Figure 1 shows the geometric model (a) and discretized model (b) used in the simulations. The model consists of a 4 m x 4 m square and a flat plate with a length of 2 m, located 0.375 m above the floor, with an initial temperature of 353.15 K. The plate has different inclination angles relative to the floor (ranging from 0° to 80°, with an increment of 10° for each simulation).

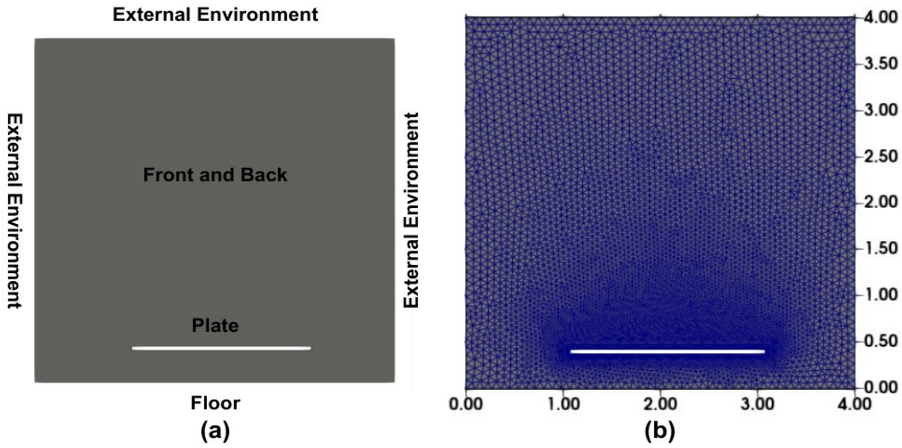

Figure 1. (a) Geometric model of the computational domain. (b) Pseudo-3D finite volume mesh.

The ambient fluid was defined as air, simulated as a perfect gas. The values of the air properties were assigned at a temperature of 298.18 K and a pressure of 1 atm [12], with a dynamic viscosity equal to $1.849\cdot10^{-5}$ kg/m·s, specific heat at constant pressure equal to 1000 J/kg·K, Prandtl number equal to 0.7296, and initial temperature equal to the uniform value of 298.15 K. The quality parameters of the generated meshes can be observed in Tab. (1).

Table 1. Characteristics of the generated finite volume meshes.

Case	Total number of cells	Max aspect ratio	Non-orthogonality		Max skewness
			Max	Average	
Tilted Plate 0°	15074	16.5131	44.7389	16.2681	2.00191
Tilted Plate 10°	15383	4.68476	44.8150	16.1436	2.00289
Tilted Plate 20°	15755	2.68321	44.8942	15.9530	2.00242
Tilted Plate 30°	15949	2.33159	44.9837	15.8733	2.00274
Tilted Plate 40°	15851	2.34579	44.9423	15.9637	2.00533
Tilted Plate 50°	15844	2.12509	44.9187	15.9176	2.00267
Tilted Plate 60°	16002	2.17391	44.8795	15.8895	2.00299
Tilted Plate 70°	15746	2.68347	44.8260	15.9835	2.00230
Tilted Plate 80°	15698	4.68542	44.8468	16.0359	2.00349

In CFD, y+ is a dimensionless distance from the wall, defined as a measure of the position of the first mesh cell relative to the wall, and is used to assess the accuracy of turbulence models near solid boundaries [13]. For the simulations, the y+ values, obtained through a function object in OpenFOAM, ranged between 6 and 0.5.

For the processing stage, OpenFOAM offers a variety of solvers for different types of flows. The transient solver buoyantPimpleFoam was used for single-phase, buoyant, and turbulent compressible fluid flows for heat transfer, incorporating the K-epsilon turbulence model. The turbulence model introduces two transport equations, one for turbulent kinetic energy (k) eq. (5) and another for the dissipation rate of turbulent kinetic energy (ϵ) eq. (6). These equations are used to determine the value of turbulent viscosity, defined in eq. (7), which is then followed by solving the Reynolds stresses [14].

$$\frac{\partial(\rho k)}{(\partial t)}+\nabla\cdot(\rho k V)=\nabla\cdot\left[\frac{\mu_t}{\sigma_k}\nabla k\right]+2\mu_t S_{ij}\cdot S_{ij}-\rho\epsilon \tag{5}$$

$$\frac{\partial(\rho\epsilon)}{(\partial t)}+\nabla\cdot(\rho\epsilon V)=\nabla\cdot\left[\frac{\mu_t}{\sigma_\epsilon}\nabla\epsilon\right]+C_{1\epsilon}\frac{\epsilon}{k}\mu_t S_{ij}\cdot S_{ij}-C_{2\epsilon}\rho\frac{\epsilon^2}{k} \tag{6}$$

$$\mu_t=\rho C_\mu\frac{k^2}{\epsilon} \tag{7}$$

With the standard coefficient values: $C\mu = 0.09$; $\sigma k = 1.0$; $\sigma\epsilon = 1.3$; $C1\epsilon = 1.44$; $C2\epsilon = 1.92$.

For solving the pressure-velocity coupling, the solver utilizes the PIMPLE algorithm, a blend of the PISO (Pressure-Implicit with Splitting of Operators) and SIMPLE (Semi-Implicit Method for Pressure Linked Equations) methods. It's an iterative algorithm that uses corrected pressure and corrected velocity equations, obtained from the continuity or Poisson equation for pressure, to ensure mass conservation and robustness in treating transient flows with large time steps [15].

In OpenFOAM, the fvSchemes dictionary is used to define the numerical schemes employed in the discretization of partial differential equations. For the simulations, the following were used: the Euler method for discretizing first-order derivatives; Gaussian integration with linear interpolation for gradient terms; Gaussian integration with both linear interpolation and upwind interpolation for divergence terms; the Gauss scheme with linear interpolation for the diffusion coefficient and a corrected scheme for the surface normal gradient; linear interpolation for cell face values based on cell center values; and the corrected scheme with under-relaxation applied for calculating surface normal gradient terms.

The controls for algorithms and solvers are found in the fvSolution dictionary. For the simulations, the following were used: the preconditioned conjugate gradient (PCG) solver for symmetric matrices and the preconditioned biconjugate gradient stabilized (PBiCGStab) solver for asymmetric matrices, with incomplete Cholesky and incomplete LU diagonal-based preconditioners; solver tolerances in the range of $1\cdot10^{-6}$ to $1\cdot10^{-8}$; and relative solver tolerance values of 0.01 for initial resolutions and 0 for the final resolution of each iteration. For the PIMPLE algorithm, two steps for pressure correction were defined in nCorrectors. The simulations were performed in transient state with a final time of 80 seconds and a time step value of $1\cdot10^{-3}$, a parameter adjusted to keep the Courant number below 0.5. This was monitored through the simulation log.

For each of the domain surfaces defined in the mesh, initial and boundary conditions were assigned [16]. Table (2) presents these conditions for the temperature (K), velocity (m/s), hydrostatic pressure (kg/m·s²), pressure (kg/m·s²), turbulent viscosity (m²/s), turbulent kinetic energy (m²/s²), turbulent kinetic energy dissipation rate (m²/s³), and turbulent thermal diffusivity (m²/s).

Table 2. Initial conditions and boundary conditions for 2D simulations.

	Front and Back	**Plate**	**Floor**	**External Environment**
T (K)	empty	FixedValue value uniform 353.15	zeroGradient	zeroGradient
U (m/s)	empty	noSlip	noSlip	PressureInletOutletVelocity value uniform (0 0 0)
p_rgh (kg/m·s²)	empty	FixedFluxPressure value uniform 0	FixedFluxPressure value uniform 0	TotalPressure p0 uniform 0
p (kg/m·s²)	empty	Calculated value uniform 100000	Calculated value uniform 100000	Calculated value uniform 100000
nut (m²/s)	empty	NutkWallFunction value uniform 0	NutkWallFunction value uniform 0	zeroGradient
k (m²/s²)	empty	KqRWallFunction value uniform 0.1	KqRWallFunction value uniform 0.1	zeroGradient
epsilon (m²/s³)	empty	EpsilonWallFunction value uniform 0.01	EpsilonWallFunction value uniform 0.01	zeroGradient

alphat (m^2/s)	empty	compressible::alphatWall Function value uniform 0	compressible::alphatWall Function value uniform 0	zeroGradient

3 Results and discussions

Upon completing the CFD modeling, the post-processing is the stage of analyzing the numerical results obtained during the processing stage. For this, the software Paraview [17] was used. Figure 2 (a) shows the temperature variation over time for the case of the heated horizontal flat plate in a natural convection regime. The results show the formation of flows and the gradual propagation of temperature into the environment from the plate. This occurs due to the fluid movement resulting from buoyancy forces inside, which arise from the density gradient. The fluid near the photovoltaic, with a high temperature, rises due to the reduction in density and drags the surrounding fluid. As it moves away from the plate, it dissipates due to cooling, a phenomenon known in the literature as a thermal plume.

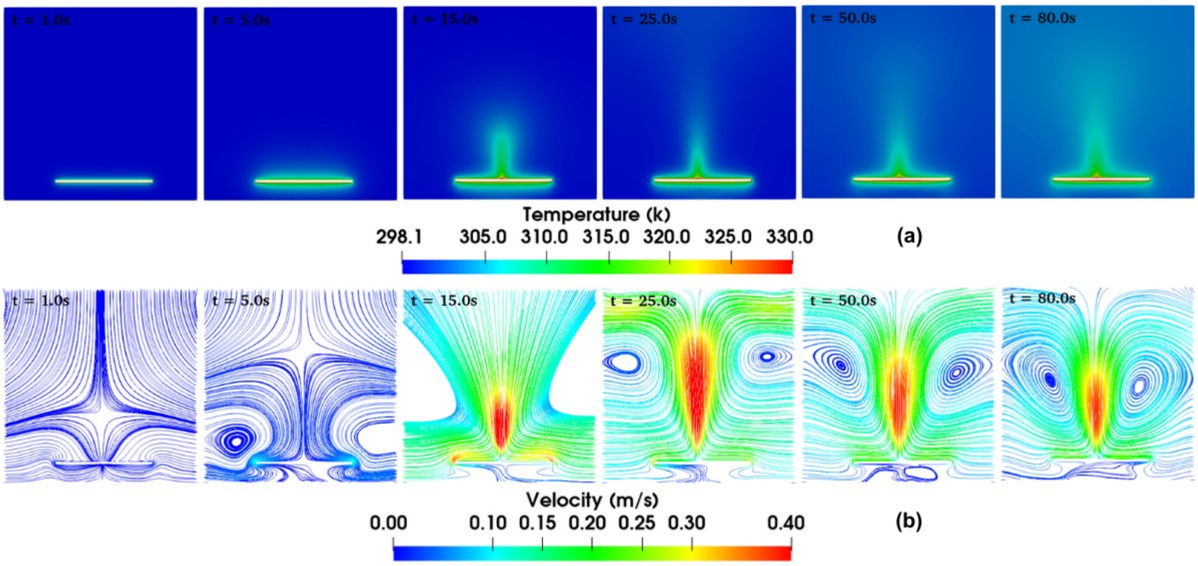

Figure 2. (a) Variation of the temperature field over time for the horizontal plate case. (b) Variation of the velocity field and air flow lines over time.

Natural convection caused the formation of air flows in the environment due to the buoyancy effects that occur with the variation in the fluid's density. Figure 2 (b) shows the visualization of the velocity field for the case of the heated horizontal flat plate, where it is possible to see the formation of air recirculation patterns with the assistance of the Paraview tool "streamtracer".

Figure 3 (a) presents a comparison of the temperature field results of the flow for different inclination angles of the flat plate, with results for the last calculated time step. It is observed that the thermal plumes displaced towards the inclination of the plate, which influenced the velocity profile found in the convection. Additionally, there was an increase in the average temperature of the environment around the plate with the increase in the photovoltaic inclination angle. Figure 3 (b) presents a comparison of the air displacement flows for different inclinations of the plate, with results for the last calculated time step. It is possible to notice the interference that the angle of the plate has, thus forming different patterns of air recirculation over time in the vicinity of the plate, interfering with the turbulence phenomena.

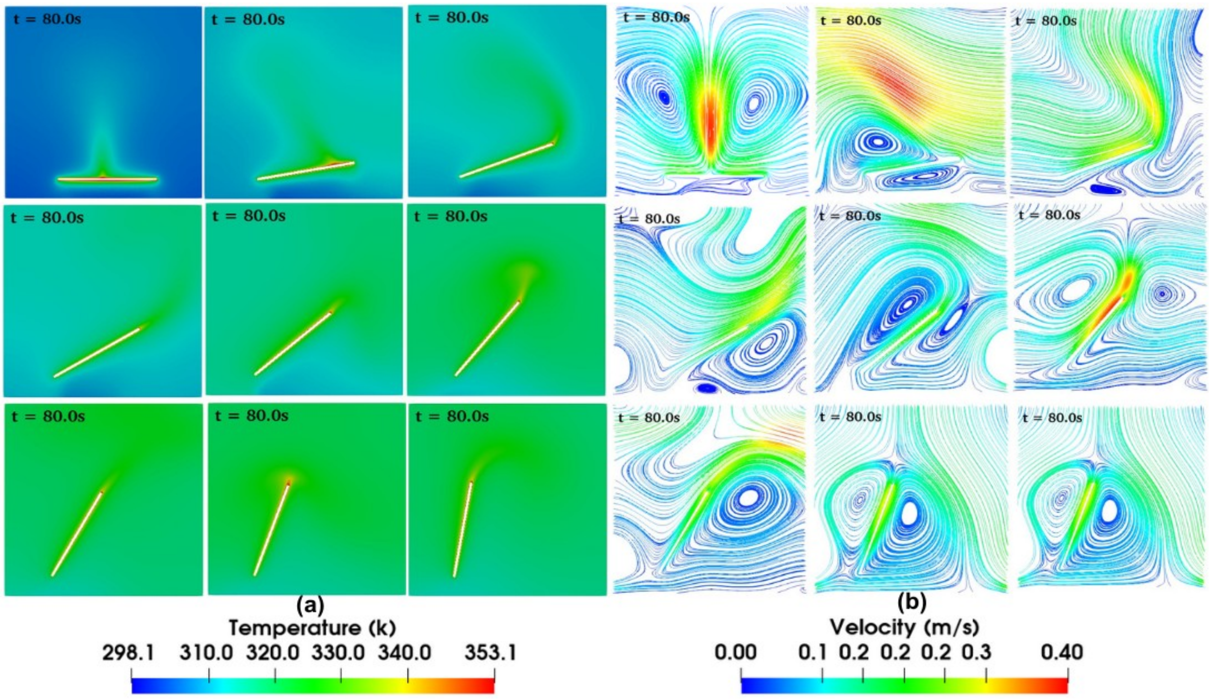

Figure 3. (a) Comparison of the temperature field for the different slopes. (b) Comparison of air flow lines for different inclinations.

For better visualization of the temperature increase, Fig. 4 presents comparative graphs of the fluid temperature for different plate inclinations at vertical distances of 3.5 m (a), 2.5 m (b), and 1.5 m (c) from the ground. At a height of 3.5 meters from the ground, there was an increase in the average temperature for inclination ranges from 0° to 60°; for inclinations above 60°, there was a slight decrease in the average temperature. The difference in average temperature between the case with the lowest (horizontal plate – average temperature of 302.89 K) and highest temperature (plate inclined at 60° – average temperature of 312.26 K) found at a height of 3.5 meters from the ground was approximately 10 K.

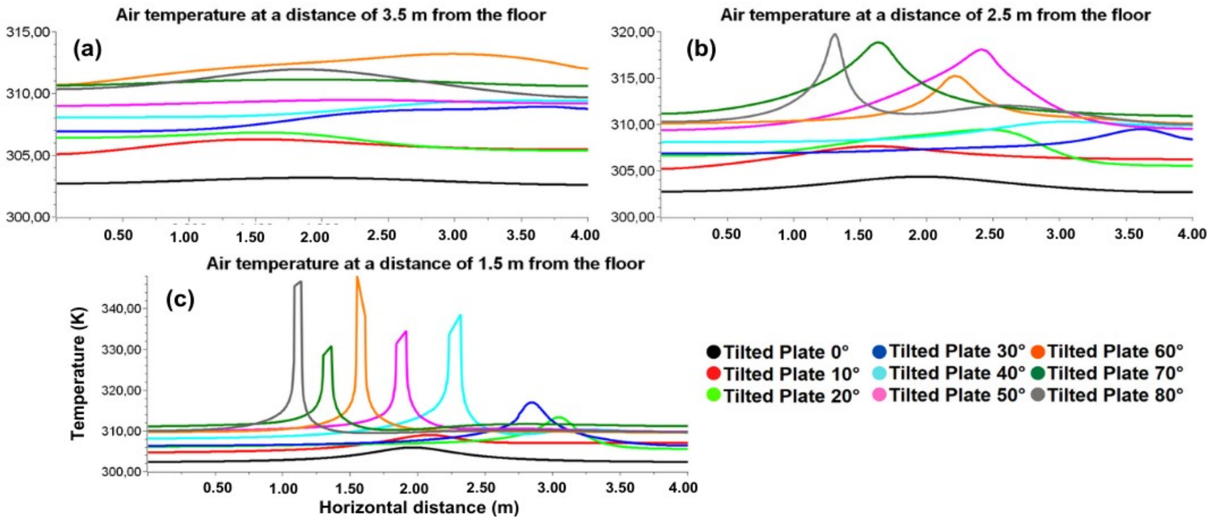

Figure 4. Comparison of fluid temperature values for different inclinations at vertical distances of 3.5 m (a), 2.5 m (b), and 1.5 m (c) from the ground.

The results from Fig. 3 and Fig. 4 are corroborate with what is reported in the literature. Guha et al. [18], using the commercial software FLUENT to model the behavior of a uniformly heated plate transitioning from a horizontal to a vertical position, found that the Nusselt number initially decreases slightly and then continuously increases until reaching the vertical position of the plate. Abdulateef [19] used the finite difference method to solve the conservation equations for the natural convection problem in a square flat plate with varying inclination angles. The results presented by the author indicate that the Nusselt number reaches its maximum value at the vertical position, reporting increases of up to 20%.

4 Conclusions

The results obtained show the formation of air flows and the gradual propagation of temperature to the external environment from the plate through thermal plumes. It is observed from the simulations that the increase in the plate inclination relative to the ground contributes to the increase in the average temperature of the environment around the plate. The importance of the numerical solution of fluid flow, which enabled this study, is highlighted, as it eliminates the main obstacles of experimental analysis such as the high cost of obtaining materials and the difficulty of controlling external simulation factors. Moreover, the free software used in the methodology is emphasized. OpenFOAM allows the user to control and modify the simulation parameters, the finite volume discretization schemes, and the linear system resolution method, thus having a positive impact on learning. This enables the exploration of various research fronts in the field of CFD.

Acknowledgements. This work was carried out with funding from the Federal University of Alagoas (UFAL) through a scholarship in the Scientific Initiation (IC) modality.

Authorship statement. The authors hereby confirm that they are the sole liable persons responsible for the authorship of this work, and that all material that has been herein included as part of the present paper is either the property (and authorship) of the authors, or has the permission of the owners to be included here.

References

[1] Pereira, E. B., Martins, F. R., Gonçalves, A. R., Costa, R. S., Lima, F. J. L. D., Rüther, R., ... & Souza, J. G. D. (2017). Atlas brasileiro de energia solar (Vol. 2). São José dos Campos: INPE.
[2] Oliveira, J. G. G. D. (2018). Convecção mista em painéis fotovoltaicos (Dissertação de Mestrado). Departamento de Engenharia Mecânica, Universidade de Brasília, Brasília, Brasil.
[3] Saleem, A., Iqbal, A., Hayat, M. A., Panjwani, M. K., Mangi, F. H., & Larik, R. M. (2020). The effect of environmental changes on the efficiency of the PV system. Indonesian Journal of Electrical Engineering and Computer Science, 18(1), 558-564.
[4] Amelia, A. R., Irwan, Y. M., Leow, W. Z., Irwanto, M., Safwati, I., & Zhafarina, M. (2016). Investigation of the effect temperature on photovoltaic (PV) panel output performance. Int. J. Adv. Sci. Eng. Inf. Technol, 6(5), 682-688.
[5] ižetić, S., Marinić-Kragić, I., Grubišić-Čabo, F., Papadopoulos, A. M., & Xie, G. (2020). Analysis of novel passive cooling strategies for free-standing silicon photovoltaic panels. Journal of Thermal Analysis and Calorimetry, 141, 163-175.
[6] Fan, Y., Zhao, Y., Torres, J. F., Xu, F., Lei, C., Li, Y., & Carmeliet, J. (2021). Natural convection over vertical and horizontal heated flat surfaces: A review of recent progress focusing on underpinnings and implications for heat transfer and environmental applications. Physics of Fluids, 33(10).
[7] Jaffer, A. (2023). Natural convection heat transfer from an isothermal plate. Thermo, 3(1), 148-175.
[8] OPENFOAM. User Guide v2112: the open source cfd toolbox. Available at: https://www.openfoam.com/documentation/guides/v2112/doc/.
[9] White, F. M. (2010). Mecânica dos fluidos. 6. ed. Editora McGraw Hill.
[10] Maliska, C. R. (2017). Transferência de calor e mecânica dos fluidos computacional. Grupo Gen-LTC.
[11] GMSH. A three-dimensional finite element mesh generator with built-in pre- and postprocessing facilities. Available at: https://gmsh.info/#Documentation.
[12] Cengel, Y. A., & Cimbala, J. M. (2015). Mecânica dos fluidos-3. Amgh Editora.
[13] SIMSCALE. What is y+ (yplus)? 2018. Disponível em: https://www.simscale.com/forum/t/what-is-y-yplus/82394. Acesso em: 12 set. 2024.
[14] Ito, M. C. (2020). Avaliação numérico-experimental da convecção natural em uma placa plana horizontal.
[15] Versteeg H. K., Malalasekera, W. (2007). An introduction to computational fluid dynamics: the finite volume method. Pearson Prentice Hall.
[16] CFD Monkey. A brief explanation of boundary conditions in OpenFOAM. 2024. Available at: https://cfdmonkey.com/a-brief-explanation-of-boundary-conditions-in-openfoam/.
[17] PARAVIEW. ParaView Documentation. Available at: https://docs.paraview.org/en/latest/.
[18] Guha, A., Jain, A., & Pradhan, K. (2019). Computation and physical explanation of the thermo-fluid-dynamics of natural convection around heated inclined plates with inclination varying from horizontal to vertical. International Journal of Heat and Mass Transfer, 135, 1130-1151.
[19] Abdulateef, J., & Hassan, A. (2015). Correlations for Nusselt number in free convection from an isothermal inclined square plate by a numerical simulation. American Journal of Mechanics and Applications, 3(2), 8-18.